Higher Order Generalized Thermoelastic Model with Memory Responses in Nonhomogeneous Elastic Medium due to Laser Pulse

SOUMEN SHAW[1,*], AKTAR SEIKH[2]
[1]Department of Mathematics,
Dinabandhu Andrews College, Kolkata-700084,
INDIA

[2]Indian Institute of Engineering Science and Technology,
Shibpur, Howrah-711103,
INDIA

*Corresponding Author

Abstract: - The present article deals with the thermoelastic behavior of a nonhomogeneous isotropic material. This study is carried out in the context of an advanced thermoelastic model involving a higher order memory dependent derivative (MDD) with dual time delay terms. The thermoelastic interactions and evolved stresses into the medium are analyzed subject to external mechanical load as well as laser-type heat source. It is observed that the material moduli of the medium have a significant impact on its thermodynamic behavior. The analytical expression of the field functions is obtained in the integral transform domain. To know the nature of the field functions in the space-time domain, a discretized form of the inverse integral transformations is applied and depicted graphically for various kernel functions and empirical constants.

Key-Words: - Nonhomogeneous medium, memory-dependent derivative, fractional derivative, generalized thermoelasticity, material moduli, continuous load, instantaneous load.

Received: April 14, 2023. Revised: February 17, 2024. Accepted: March 11, 2024. Published: April 17, 2024.

1 Introduction

A conventional method that has been widely used to investigate the thermoelastic behavior of a material is Fourier's law of heat conduction. Even though Fourier's law is well established, it predicts the infinite speed of propagation of thermal signals, and one of its potential drawbacks is its accuracy, which leads to failure in situations involving incredibly low temperatures, extremely high heat flow, and very short periods. To surmount the drawbacks, various modified generalized thermoelasticity models have been introduced. The hyperbolic type heat transport equation present in generalized thermoelasticity theory predicts that thermal signals will propagate with a finite speed in a wavelike fashion. Numerous generalized thermoelasticity models have been developed by different researchers, the widely acceptable models are mentioned in the articles, [1], [2], [3], [4], [5], [6], [7], etc. Under different kinds of circumstances, the unique property of the solutions was established by many researchers, [8], [9], [10]. The monograph, [11], describes a brief history of generalized thermoelasticity. The Dual-phase lag model, which was proposed by Tzou, is one of these newly presented models. [12], introduced a three phase lag generalized thermoelasticity model. Recently, a modified G-L theory with strain rate has been introduced in the article [13] and a modified L-S theory with decomposed heat flux has been introduced in [14].

Non-homogeneous properties of the material moduli played an important role in the field of mechanics. Variation in temperature distribution is another significant domain and received great attention in the industry connection with the rapid growth of society. Material response at low temperatures and at high flux rates is extremely important in fields like the aviation industry, nuclear explosion, etc. In the thermoelastic domain, most of the researchers studied deformation and temperature distribution based on the medium having constant material moduli. Discarding the influence of elastic deformation of the medium as well as the temperature variations on the material moduli leads the analysis towards a smaller region in terms of applicability. Practically, the material moduli viz., modulus of elasticity, thermal conductivity, and coefficient of linear thermal expansion is no longer constant in the high-temperature range, [15]. By considering temperature-dependent properties, Noda, in his article [16], examined the characteristics of thermal stresses in a thermoelastic material. [17], dealt with a generalized thermoelastic problem by taking the dependency of material moduli on the reference temperature. The [18], reports that mechanical rigidity and chemical inertness varies with the temperature dependence of Young's modulus of a single-crystal diamond. Furthermore, Young's modulus of a Si-crystal plays an important role in determining thermal stress inside the ingot during the cooling process for crystal growth, [19].

In 2014, implementing the idea of derivatives with sleeping intervals, Wang and Li developed the idea of memory-dependent derivative in the generalized thermoelasticity in terms of the fractional derivative due to [20], [21], [22]. In this modern generalized thermoelasticity model, the time delay factor is conveniently used as the length of the slipping time interval. The first order memory dependent derivative can be expressed as an integral form of a common derivative using a freely chosen kernel function $k(t-\xi)$ on the sliding interval $[t-\tau,t]$ as follows:

$$D_\tau f(t) = \frac{1}{\tau}\int_{t-\tau}^{t} k(t-\xi) f(\xi) d\xi,$$

where $\tau > 0$ is the time delay.

Memory-dependent derivatives outperform fractional order generalized thermoelasticity at establishing the memory effect (the preceding state affects the immediate rate of change). It is simple to define in terms of the physical environment, and the memory-dependent differential equation signifies a higher level of expressiveness.

The heat transport equation has been modified in the perspective of MDD. The differential equations that emerge from using memory-dependent methods are more effective in practical applications because the definition of MDD is more intuitive in how physical importance is observed. Other efforts have recently been attempted to modify the conventional Fourier law to improve on earlier models using governing equations that incorporate higher-order derivatives. In 2021, based on MDD, a new model of generalized thermoelasticity has been proposed by considering the time delay factor, [23]. An advanced model in the field of thermoelasticity from the perspective of higher order MDD with dual time delay factors has been introduced in [24]. The Memory-dependent derivatives in magneto-thermoelastic transversely isotropic media with two temperatures has been discussed in [25]. The impacts of stiffness and memory on energy ratios at the interface of different media have been investigated in [26]. Thermal wave propagation in an unbounded medium with a cavity has been discussed in [27]. Recently published few articles have shown significant developments in-terms of capturing the nonlocal response of the materials, [28], [29], [30], [31], [32], [33], [34].

Moreover, several aspects of the thermoelastic medium have been studied in [35], [36], [37], [38], [39], [40]. Modified Moore–Gibson–Thompson on rotating semiconductors and on orthotropic hollow-cylinder have been studied in the articles [41], [42].

Recently quick thermal processes using an ultra-short laser pulse are receiving attention from a thermoelasticity viewpoint. The primary reason for this attraction is that it requires a study of the coupled temperature and deformation fields. This suggests that the energy absorption of the laser pulse causes a localized temperature increase that causes thermal expansion and prompts fast reactions inside the structure of the elements, increasing the vibration of the structure. There have been several significant studies on the impact of laser pulses on generalized thermoelasticity, some of which are given in [43], [44], [45], [46].

The main objective of the present article is to analyze the impact of the inhomogeneity of material characteristics interacting with generalized thermoelastic models containing higher order memory dependent derivatives. The homogeneity of the medium varies in the form of variable material moduli. The nature of the deformations and distribution of the temperature are predicted through this present analysis. The variation of stresses, displacement, and temperature are depicted graphically for different kernel functions and empirical constants.

2 Statement of the Problem

In the present problem, we are taking into consideration a thermoelastic problem for an isotropic medium with a laser pulse heat source in the $x_1 - x_3$ plane.

The constitutive equation: The stress-strain-temperature relation is given by [11],

$$\tau_{ij} = \left(\lambda\epsilon_{kk} - \gamma\hat{T}\right)\delta_{ij} + 2\mu\epsilon_{ij} \tag{1}$$

The equation of motion: The equation of motion in absence of body force is given by [11],

$$\tau_{ij,j} = \rho\ddot{u}_i \tag{2}$$

The heat conduction equation: The generalized heat conduction equation from the perspective of higher order memory-dependent derivative with dual time delay factors as given in [24] is:

$$k\left(1 + \sum_{p=1}^{N_1} \frac{\tau_\theta^p}{p!} D_{\tau_\theta}^p\right)\nabla^2 T = \left(1 + \sum_{p=1}^{N_2} \frac{\tau_q^p}{p!} D_{\tau_q}^p\right)\left(\rho C_v \dot{T} + \gamma T_0 \dot{\epsilon}_{kk} - \rho Q\right), \tag{3}$$

we shall take the heat Q input as given in [47].

$$Q(x_1, x_3, t) = I_0 J(t) g_1(x_1) g_2(x_3), \tag{4}$$

where

$$g_1(x_1) = \frac{1}{2\pi r_1^2}\exp\left(-\frac{x_1^2}{r_1^2}\right), \quad g_2(x_3) = \nu_0 \exp(-\nu_0 x_3), \quad J(t) = \frac{t}{t_0^2}\exp\left(-\frac{t}{t_0}\right). \tag{5}$$

Here r_1, *and* v_0 are the radius of the beam and absorption depth of heating energy respectively.
The operator $D_{\tau_i}^p f(t)$ is defined as:

$$D_{\tau_i}^p f(t) = \frac{1}{\tau_i}\int_{t-\tau_i}^{t} k(t-\xi) f^p(\xi)\, d\xi, \tag{6}$$

with the kernel function $k(t-\xi)$ as:

$$k(t-\xi) = 1 - \frac{2a}{\tau_i}(t-\xi) + \frac{b^2}{\tau_i^2}(t-\xi)^2 = \begin{cases} 1 & if\ b = 0,\ a = 0 \\ 1 - \frac{t-\xi}{\tau_i} & if\ b = 0, a = 1/2 \\ \left[1 - \frac{t-\xi}{\tau_i}\right]^2 & if\ b = 1, \quad a = 1 \end{cases} \tag{7}$$

where ϵ_{ij} is the strain component defined as: $\epsilon_{ij} = \frac{1}{2}(u_{i,j} + u_{j,i})$, δ_{ij} is Kronecker delta, $\gamma = (3\lambda + 2\mu)\alpha_t$, λ and μ are material moduli, α_t is the coefficient of thermal expansion, τ_{ij} is the stress component, T is the absolute temperature, T_0 is reference temperature, $\hat{T} = T - T_0$, ρ is the material density, k is the coefficient of thermal conductivity, τ_θ, and τ_q are two-time delay factors. For the detailed discussion about the heat conduction models on kernel functions, [48].

The equation (3) is simpler to comprehend in terms of its physical significance, and the equivalent differential equations based on memory dependence have stronger expressive capabilities. When $N_1 = N_2$, it represents a diffusive behavior, and when $N_2 = N_1 + 1$ it explains a wave behavior. For $N_1 = 1$ and $N_2 = 2$, it gives a dual phase-lags model. In this case, the system is exponentially stable when $\tau_q < 2\tau_\theta$ and unstable when $\tau_q > 2\tau_\theta$. For $N_1 = 2$ and $N_2 = 2$, it also represents a dual phase-lags model. In this case, the system is exponentially stable when $\tau_q > (2 - \sqrt{3})\tau_\theta$. Thus, the values of the parameters N_1 and N_2 are not allowed to be selected arbitrarily but rather accurately depending upon their stability.

3 Governing Equations

We shall consider the material moduli in the way described below as given in [49].

$$\gamma = \gamma_t g(T),\ \mu = \mu_t g(T),\ \lambda = \lambda_t g(T) \tag{8}$$

where $g(T)$ is a dimensionless function of temperature given by:

$$g(T) = 1 - \alpha^* T_0 \tag{9}$$

where the α^* is the empirical material constant when $\alpha^* = 0$ it implies temperature independent material moduli.

Now by introducing (1) and (8) in equation (2) we have the following equations of motion:

$$b_1\frac{\partial^2 u_1}{\partial x_1^2} + b_2\frac{\partial^2 u_3}{\partial x_1 \partial x_3} + \mu_t g(T)\frac{\partial^2 u_1}{\partial x_3^2} - \gamma_t g(T)\frac{\partial \hat{T}}{\partial x_1} = \rho\frac{\partial^2 u_1}{\partial t^2} \tag{10}$$

where

$$b_1\frac{\partial^2 u_3}{\partial x_3^2} + b_2\frac{\partial^2 u_1}{\partial x_1 \partial x_3} + \mu_t g(T)\frac{\partial^2 u_3}{\partial x_1^2} - \gamma_t g(T)\frac{\partial \hat{T}}{\partial x_3} = \rho\frac{\partial^2 u_3}{\partial t^2}$$

$$b_1 = g(T)(\lambda_t + 2\mu_t), \quad b_2 = g(T)(\lambda_t + \mu_t) \tag{11}$$

We shall take the dimensionless quantities as follows:

$$(x_1', x_3', \nu', r_1', u_1', u_3') = c_0\eta(x_1, x_3, \nu, r_1, u_1, u_3), \ (t', \tau_\theta', \tau_q', t_0') = c_0^2\eta(t, \tau_\theta, \tau_q, t_0)$$
$$\tau_{ij}' = \frac{\tau_{ij}}{\mu}, \quad \theta = \frac{\gamma\hat{T}}{b_1}, \quad I_0' = \frac{c_0\eta}{\rho C_v T_0} I_0 \tag{12}$$

where

$\eta = \frac{\rho C_v}{k}$, ${c_0}^2 = \frac{b_1}{\rho}$

By introducing (12) in equations (10) and (11) the following equations are obtained:

$$\frac{\partial^2 u_1}{\partial x_1^2} + A_1 \frac{\partial^2 u_3}{\partial x_1 \partial x_3} + A_2 \frac{\partial^2 u_1}{\partial x_3^2} - \frac{\partial \theta}{\partial x_1} = \frac{\partial^2 u_1}{\partial t^2} \quad (13)$$

$$\frac{\partial^2 u_3}{\partial x_3^2} + A_1 \frac{\partial^2 u_1}{\partial x_1 \partial x_3} + A_2 \frac{\partial^2 u_3}{\partial x_1^2} - \frac{\partial \theta}{\partial x_1} = \frac{\partial^2 u_3}{\partial t^2} \quad (14)$$

where $A_1 = \frac{(\lambda_* - \mu_*) g(T)}{\rho c_0^2}$ and $A_2 = \frac{\mu_* g(T)}{\rho c_0^2}$

The nondimensional form of the heat conduction equation (3) becomes:

$$\left(1 + \sum_{p=1}^{N_1} \frac{\tau_\theta^p}{p!} D_{\tau_\theta}^p\right) \nabla^2 \theta = \left(1 + \sum_{p=1}^{N_2} \frac{\tau_\theta^p}{p!} D_{\tau_\theta}^p\right) \left(\dot{\theta} + l_0 \nabla^2 \dot{\phi} - \frac{l_1 t}{t_0} e^{-\frac{x_1^2}{r_1^2} - \frac{t}{t_0} - b_0 x_3}\right) \quad (15)$$

where

$l_0 = \frac{\gamma^2 T_0}{\rho C_v b_1}$, $l_1 = \frac{\gamma T_0 I_0 \nu_0}{2\pi r_1^2 b_1 t_0 c_0^2 C_v}$, $b_0 = \frac{\nu_0}{c_0^2 \eta^2}$

Now we shall introduce the potential functions ϕ and ψ as follows:

$$u_1 = \frac{\partial \phi}{\partial x_1} + \frac{\partial \psi}{\partial x_3}$$
$$u_3 = \frac{\partial \phi}{\partial x_3} - \frac{\partial \psi}{\partial x_1} \quad (16)$$

By introducing (16) in the equations (13),(14), and (15) we obtained the following system of equations:

$$\frac{\partial^2 \phi}{\partial t^2} = \nabla^2 \phi - \theta, \quad (17)$$

$$\frac{\partial^2 \psi}{\partial t^2} = A_2 \nabla^2 \psi, \quad (18)$$

$$\left(1 + \sum_{p=1}^{N_1} \frac{\tau_\theta^p}{p!} D_{\tau_\theta}^p\right) \nabla^2 \theta = \left(1 + \sum_{p=1}^{N_2} \frac{\tau_\theta^p}{p!} D_{\tau_\theta}^p\right) \left(\dot{\theta} + l_0 \nabla^2 \dot{\phi} - \frac{l_1 t}{t_0} e^{-\frac{x_1^2}{r_1^2} - \frac{t}{t_0} - b_0 x_3}\right) \quad (19)$$

where $\nabla^2 \equiv \frac{\partial^2}{\partial x_1^2} + \frac{\partial^2}{\partial x_3^2}$.

Now we shall introduce the Laplace transform defined as:

$$\bar{f}(x_1, x_2, s) = \int_0^\infty f(x_1, x_2, t) e^{-st} dt \quad (20)$$

By applying the Laplace transform to the memory-dependent derivative $D_{\tau_i}^p$ we have:

$$\mathcal{L}\left[\tau_i D_{\tau_i}^p f(t)\right] = \mathcal{L}\left[\int_{t-\tau_i}^t k(t-\xi) f^p(\xi) d\xi\right] = s^{p-1} G(s, \tau_i) \bar{f}(s) \quad (21)$$

where

$$G(s, \tau_i) = (1 - e^{-s\tau_i})\left(1 - \frac{2a}{\tau_i s} + \frac{2b^2}{\tau_i^2 s^2}\right) - e^{-s\tau_i}\left(b^2 - 2a + \frac{2b^2}{\tau_i s}\right) \quad (22)$$

Now by taking the Laplace transform on both sides of equations(17),(18), and(19) and considering homogeneous initial conditions the following system of equations is obtained :

$$s^2 \bar{\phi} = \nabla^2 \bar{\phi} - \bar{\theta} \quad (23)$$

$$s^2 \bar{\psi} = A_2 \nabla^2 \bar{\psi} \quad (24)$$

$$d_1 \nabla^2 \bar{\theta} = d_2 \left(s\bar{\theta} + l_0 s \nabla^2 \bar{\phi} - l_1 g_1(s) \exp\left(-\frac{x_1^2}{r_1^2}\right) \exp(-b_0 x_3)\right), \quad (25)$$

$d_1 = 1 + \sum_{p=1}^{N_1} \frac{\tau_\theta^p}{p!} s^{p-1} G(s, \tau_\theta)$, $d_2 = 1 + \sum_{p=1}^{N_2} \frac{\tau_q^p}{p!} s^{p-1} G(s, \tau_q)$, $g_1(s) = \frac{t_0}{(t_0 s + 1)^2}$

Now we shall use the Fourier transform as described below:

$$\tilde{f}(\zeta, x_3, s) = \int_{-\infty}^{\infty} \bar{f}(x_1, x_3, s) e^{i\zeta x_1} dx_1 \quad (26)$$

By applying the Fourier transform on both sides of equations (23), (24) and (25) we obtained the following system of equations:

$$(D^2 + E_1)\tilde{\phi} - \tilde{\theta} = 0, \quad (27)$$

$$(D^2 + E_2)\tilde{\psi} = 0, \quad (28)$$

$$(D^2 - d_3)\tilde{\theta} = d_4 (D^2 - \zeta^2)\tilde{\phi} - d_5 F(\zeta) exp(-b_0 x_3), \quad (29)$$

where

$D \equiv \frac{d}{dx_3}$, $E_1 = -(\zeta^2 + s^2)$, $E_2 = -\left(\zeta^2 + \frac{s^2}{A_2}\right)$, $d_3 = -\left(\zeta^2 + \frac{d_2 s}{d_1}\right)$, $d_4 = \frac{d_2 l_0 s}{d_1}$, $d_5 = \frac{l_1 g_1(s)}{d_1}$, $F(\zeta) = r_1 \sqrt{\pi} exp\left(-\frac{\zeta^2 r_1^2}{4}\right)$.

Thus, $\tilde{\phi}$ satisfies the following ODE:

$$(D^2 - m_1^2)(D^2 - m_2^2)\tilde{\phi} = d_5 F(\zeta) \exp(-b_0 x_3), \quad (30)$$

where m_1^2, m_2^2 are the roots of the equation:

$m^4 + (E_1 - d_3 + d_4)m^2 - (E_1 d_3 - d_4 \zeta^2) = 0.$

Here we assume that the solutions are bounded as $x_3 \rightarrow \infty$ and b_0^2 is not a root of the above quadratic equation of m^2. The solutions for $\tilde{\phi}$, $\tilde{\theta}$ and $\tilde{\psi}$ are obtained as:

$$\tilde{\phi}(\zeta, x_3, s) = \sum_{j=1}^{2} H_j exp(-m_j x_3) + d_5 F(\zeta) \frac{\exp(-b_0 x_3)}{(b_0^2 - m_1^2)(b_0^2 - m_2^2)} \quad (31)$$

DOI: 10.37394/232011.2024.19.3

$$\tilde{\theta}(\zeta, x_3, s) = \sum_{j=1}^{2} N_{1j} H_j exp(-m_j x_3) + N_{14}\exp(-b_0 x_3) \tag{32}$$

$$\tilde{\psi}(\zeta, x_3, s) = H_3 exp(-m_3 x_3), \tag{33}$$

where H_1, H_2, H_3 are arbitrary, $Re(m_j) > 0,\ j = 1, 2, 3$ and $N_{11} = m_1^2 + E_1$, $N_{12} = m_2^2 + E_1,\ m_3^2 + E_2 = 0,\ N_{14} = \frac{d_5 F(\zeta)}{(b_0^2 - m_1^2)(b_0^2 - m_2^2)}(b_0^2 + E_1)$

Now introducing (20), (26) in (16) and using (31), (33) we have the following solutions for displacement components:

$$\tilde{u}_1(\zeta, x_3, s) = -i\zeta\Big[\sum_{j=1}^{2} H_j exp(-m_j x_3) + d_5 F(\zeta)\frac{\exp(-b_0 x_3)}{(b_0^2 - m_1^2)(b_0^2 - m_2^2)}\Big] \tag{34}$$
$$-m_3 H_3 exp(-m_3 x_3),$$

$$\tilde{u}_3(\zeta, x_3, s) = -\Big[\sum_{j=1}^{2} m_j H_j exp(-m_j x_3) + d_5 F(\zeta)\frac{b_0\exp(-b_0 x_3)}{(b_0^2 - m_1^2)(b_0^2 - m_2^2)}\Big] \tag{35}$$
$$+i\zeta H_3 exp(-m_3 x_3)$$

The nondimensional forms of shearing stress τ_{13} and normal stress τ_{33} are:

$$\tau_{13} = \frac{\partial u_1}{\partial x_3} + \frac{\partial u_3}{\partial x_1} \tag{36}$$

$$\tau_{33} = \frac{1}{\mu}\Big[b_1\frac{\partial u_3}{\partial x_3} + \lambda\frac{\partial u_1}{\partial x_1} - b_1\theta\Big] \tag{37}$$

Introducing (20), (26) in (36), (37) and using (32), (34), (35) we have:

$$\tilde{\tau}_{13}(\zeta, x_3, s) = \sum_{j=1}^{2} N_{2j} H_j exp(-m_j x_3) + N_{23} H_3 exp(-m_3 x_3) + N_{24} exp(-b_0 x_3), \tag{38}$$

$$\tilde{\tau}_{33}(\zeta, x_3, s) = \sum_{j=1}^{2} N_{3j} H_j exp(-m_j x_3) + N_{33} H_3 exp(-m_3 x_3) + N_{34} exp(-b_0 x_3), \tag{39}$$

where

$N_{2j} = 2i\zeta m_j\ for j = 1, 2$, $N_{23} = n_3^2 + \zeta^2$, $N_{24} = \frac{2i\zeta b_0}{(b_0^2 - m_1^2)(b_0^2 - m_2^2)} d_5 F(\zeta$

$N_{3j} = -\frac{1}{\mu}[\lambda\zeta^2 + b_1 E_1]$, $N_{33} = \frac{i\zeta m_3}{\mu}(\lambda - b_1)$, $N_{34} = -\frac{1}{\mu}(\lambda\zeta^2 + b_1 E_1)\frac{d_5 F(\zeta)}{(b_0^2 - m_1^2)(b_0^2 - m_2^2)}$

4 Mechanical Conditions

(i) τ_{13} acting on the plane x_1 = constant, here $x_1 = 0$, along the direction of x_3 axis. (ii) τ_{33} is the longitudinal stress along x_3 axis. On the line $x_3 = 0$,

$\tau_{13} = 0$,

$\theta = 0$, (40)

$\tau_{33} = -\chi_0\delta(x_1)\chi(t)$

where χ_0 is a constant and $\delta(x_1)$ is the Dirac-delta function. It represents a point load with intensity χ_0 at the origin.

The applied mechanical loads can be characterized based on the involved functions. For example; (i) a continuous load:

$$\tau_{33} = -\chi_0 sin\Big(\frac{\pi t}{\tau}\Big), \quad 0 \le t \le \tau, \quad |\, x_1 \,| \le a.$$

(ii) a continuous point load:

$$\tau_{33} = -\chi_0\delta(x_1) sin\Big(\frac{\pi t}{\tau}\Big), \quad 0 \le t \le \tau.$$

For computational purposes, we shall consider two different forms of loads in the equation (40) on the boundary plane, as follows:

$$\chi(t) = \begin{cases} \delta(t), & for\ impact\ load \\ H(t), & for\ continuous\ load \end{cases} \tag{41}$$

where $H(t)$ is the Heaviside step function.

4.1 Continuous Load

In this case, after introducing (20), (26) in (40) we obtained the following system of equations:

$$N_{11}H_1 + N_{12}H_2 + N_{14} = 0$$
$$N_{21}H_1 + N_{22}H_2 + N_{23}H_3 + N_{24} = 0$$
$$N_{31}H_1 + N_{32}H_2 + N_{33}H_3 + N_{34} = -\frac{\chi_0}{s} \tag{42}$$

Using the matrix inverse method we have:

$$\begin{bmatrix} H_1 \\ H_2 \\ H_3 \end{bmatrix} = \begin{bmatrix} N_{11} & N_{12} & 0 \\ N_{21} & N_{22} & N_{23} \\ N_{31} & N_{32} & N_{33} \end{bmatrix}^{-1} \begin{bmatrix} -N_{14} \\ -N_{24} \\ -\frac{\chi_0}{s} - N_{34} \end{bmatrix} \tag{43}$$

4.2 Impact Load

Here, in this case, we obtain the following system of equations after introducing (20), (26) in (40):

$N_{11}H_1 + N_{12}H_2 + N_{14} = 0$
$N_{21}H_1 + N_{22}H_2 + N_{23}H_3 + N_{24} = 0$ (44)
$N_{31}H_1 + N_{32}H2 + N_{33}H_3 + N_{34} = -\chi_0$

Using the matrix inverse method we have:

$$\begin{bmatrix} H_1 \\ H_2 \\ H_3 \end{bmatrix} = \begin{bmatrix} N_{11} & N_{12} & 0 \\ N_{21} & N_{22} & N_{23} \\ N_{31} & N_{32} & N_{33} \end{bmatrix}^{-1} \begin{bmatrix} -N_{14} \\ -N_{24} \\ -\chi_0 - N_{34} \end{bmatrix} \tag{45}$$

5 Numerical Analysis

The solutions have been determined in the Laplace-Fourier transform domain and are functions of x_3, as well as the parameters s and ζ. With the help of the numerical inversion methods as described in [50], [51], the solutions of temperature, displacement components, and stress components in the physical domain are obtained numerically. Numerical simulations have been carried out based on analytically determined solutions that illustrate the nature of temperature, displacement components, and stress components.

We consider a copper-like material for the numerical purpose. The values of the used parameters are as follows, [14]:
ρ = 8954 kg/m^3, C_v = 383.1 m^2/s^2K, μ_t = 3.86 × $10^{10} N/m^2$, λ_t = 7.76 × 10^{10} N/m^2, k = 386 W/mK, α_t = 1.78 × $10^{-5} K^{-1}$, v_0 = 0.5 m^{-1}, T_0 = 293K, I_0 = $10^5 j$, r_1 = 100 μm, τ_q = 0.07s, τ_θ = 0.01s.

The nature of physical quantities for various empirical constants and kernel functions are presented graphically. For the case of various empirical constants, the kernel function is taken as b = 1, a = 1 in (7) whereas in the case of different kernel functions the empirical constants have the value α^* = 0.1, N_1 = 5, N_2 = 6.

To demonstrate the characteristics of temperature, displacement components, and stress components under continuous and impact loads in the presence of a laser pulse heat source, numerical simulations are performed.

5.1 The shearing Stress (τ_{13})

Figure 1, Figure 2, Figure 3 and Figure 4 in Appendix show how the shearing stress (τ_{13}) varies under continuous and impact load in various situations. Figure 1 and Figure 2 (Appendix) depict characteristics of shearing stress (τ_{13}) under continuous load using various kernel functions and various empirical constants respectively.

Figure 1 and Figure 2 (Appendix) clarify that the shearing stress (τ_{13}) under continuous load has a small variation in $0 \leq x_3 \leq 0.5$ and then varies highly in the region $0.5 \leq x_3 \leq 1.5$. Thereafter in the region $x_3 > 1.5$ it eventually vanishes.

Figure 3 and Figure 4 (Appendix) depict characteristics of the shearing stress (τ_{13}) under impact load using different types of kernel functions and various empirical constants respectively. Figure 3 and Figure 4 (Appendix) clarify that the shearing stress (τ_{13}) under impact load varies highly at the very bottom of the x_3 axis and then up to x_3 = 1.5 it has a significant variation. Eventually, the shearing stress (τ_{13}) converges to zero in the higher region $x_3 > 1.5$.

5.2 The Normal Stress (τ_{33})

Figure 5, Figure 6, Figure 7 and Figure 8 (Appendix) show how the normal stress (τ_{33}) varies under continuous and impact load in various situations. Figure 5 and Figure 6 (Appendix) show the characteristics of the normal stress (τ_{33}) under continuous load, respectively, using different kernel functions and empirical constants.

It is noticed from Figure 5 and Figure 6 (Appendix) that the normal stress (τ_{33}) under continuous load varies slowly in the region $0 \leq x_3 \leq 0.5$ and then it has a large variation in the region $0.5 \leq x_3 \leq 1.5$. Thereafter in the region $x_3 > 1.5$ the normal stress (τ_{33}) eventually goes to zero.

Figure 7 and Figure 8 (Appendix) depict, using different kernel functions and different empirical constants, the characteristics of the normal stress ($\tau_3$3) under impact load. It is noticed from Figure 7 and Figure 8 (Appendix) that the normal stress (τ_{33}) under impact load varies significantly in the region $0 \leq x_3 \leq 0.5$ and then it varies rapidly in the region $0.5 \leq x_3 \leq 1.5$. Thereafter in the region $x_3 > 1.5$ the normal stress (τ_{33}) eventually goes to zero.

5.3 The Displacement Component u_1

The nature of the displacement component u_1 varies under continuous load and impact load in various situations, as shown in Figure 9, Figure 10, Figure 11 and Figure 12 (Appendix).

Figure 9 and Figure 10 (Appendix) illustrate the nature of the displacement component u_1 under continuous load, respectively, using different kernel functions and different empirical constants. It is clarified from Figure 9 and Figure 10 (Appendix) that the displacement component u_1 under continuous load gradually varies in the region $0 \leq x_3 \leq 0.5$ and then variations occur quickly in $0.5 \leq x_3 \leq 1.5$. After that, the displacement component u_1 ultimately converges to zero in the higher region $x_3 > 1.5$.

From Figure 11 and Figure 12 (Appendix) it is clarified that under the impact load, the displacement component u_1 gradually decreases in the very lower region of x_3 thereafter up to x_3 = 1.5 the displacement component u_1 varies highly. After that, the displacement component u_1 ultimately converges to zero in the higher region $x_3 > 1.5$.

5.4 The Displacement Component u_3

Figure 13, Figure 14, Figure 15 and Figure 16 (Appendix) illustrate the nature of the displacement component u_3 under continuous load and impact load in various cases. Figure 13 and Figure 14 (Appendix) describe the nature of the displacement component u_3 under continuous load using different kernel functions and empirical constants, respectively.

In Figure 13 and Figure 14 (Appendix), it has been noticed that the displacement component u_3 under continuous load has a slowly varying nature in the region $0 \leq x_3 \leq 0.5$, and then a rapid variation occurs in the region $0.5 \leq x_3 \leq 1.5$. Eventually, in the higher region $x_3 > 1.5$, the displacement component u_3 converges to zero.

Figure 15 and Figure 16 (Appendix) describe the nature of the displacement component u_3 under impact load using different kernel functions and empirical constants, respectively. In Figure 15 and Figure 16 (Appendix), it has been noticed that in $0 \leq x_3 < 1$, the displacement component u_3 under impact load firstly increases to a higher magnitude thereafter it varies slowly. In $1 \leq x_3 \leq 2$, the displacement component u_3 varies rapidly thereafter in the higher region $x_3 > 2$ it finally converges to zero.

5.5 The Temperature (θ)

Figure 17, Figure 18, Figure 19 and Figure 20 (Appendix) describe the nature of the temperature (θ) varies under continuous load and impact load for various cases. Figure 17 and Figure 18 (Appendix) describe the nature of the temperature (θ) under continuous load using various kernel functions and various empirical constants, respectively.

In Figure 17 and Figure 18 (Appendix) it is observed that under continuous load, in $0 \leq x_3 \leq 0.8$ the temperature (θ) has a small variation, and then in $0.8 < x_3 \leq 1.5$ it varies rapidly. Finally, in the higher region $x_3 > 1.5$, the temperature (θ) eventually goes to zero.

Figure 19 and Figure 20 (Appendix) describe the nature of the temperature (θ) under impact load using different kernel functions and empirical constants, respectively. In Figure 17 and Figure 18 (Appendix) it is noticed that in $0 \leq x_3 \leq 0.8$ the temperature (θ) varies slowly thereafter in the region $0.8 < x_3 \leq 1.5$ it has high variation. Finally, in the higher region, $x_3 >$ 1.5 the temperature (θ) goes to zero.

5.6 Effects of Kernel Functions and Empirical Constants

The considered empirical constant and different kernel functions have their advantages in the analysis of thermal thermal deformation of the solids, [52], [53]. Three different kernel functions are used in the current study. The findings are demonstrated clearly. The identical behavior of all the thermodynamic field functions is an important and notable fact. Moreover, all the field variables depend significantly on the kernel functions as well as an empirical constant in the analysis of thermoelasticity. These findings show that different kernel function structures reflect various memory influences, allowing one to select a kernel function that improves the effects of the MDD.

6 Conclusions

In this study, a non-homogeneous thermoelastic medium under mechanical loads with a laser pulse type heat source has been considered. Non-homogeneity with temperature-dependent material moduli responses has been investigated in the context of an advanced thermoelasticity model involving dual time delay factors and higher order memory-dependent derivatives.

The evaluation of theoretical and numerical results can lead to the following conclusions:

i) The kernel functions and empirical constants have a significant impact on the physical quantities, therefore their selection can be made on the situation as well as the requirement.
ii) In the case of instantaneous load (impact load), when values of the elastic moduli are decreased deformations and temperature fluctuations increase. Thus, the values of the materials' elastic moduli are inversely proportional to the entropy changes of the system. In the case of continuous load, this phenomenon is observed steadily.
iii) All of the computed results indicate that the physical quantities are non-zero in a finite zone and converge to zero at the outside of that region. This property of the physical quantities leads to the characteristics of the behavior of the hyperbolic type thermoelasticity models.
iv) Thermoelastic model with Non-linear kernel function can predict more accurate values of the field functions.

v) Higher-order differential parameters have a considerable influence on all of the field variables under investigation.

The present study may be applicable in various fields in the aviation industry and places where the deformation of the medium varies widely with temperature. This analysis can be extended in the nonlinear deformation of continuum solid as well as non-Fourier thermal conduction environment.

References:

[1] H. Lord and Y. Shulman (1967), "A generalized dynamical theory of thermoelasticity", *J. Mech. Phys. Solid*, 15(5), 299–309.

[2] Green AE and Lindsay KA (1972), "Thermoelasticity", *J. Elast.*, 2(1), 1–7.

[3] Green, A. E. and Naghdi, P. M. (1991), "A Re-examination of the Basic Postulates of Thermomechanics". *Proceedings of the Royal society*, London A, 432(1885), 171–194.

[4] A. E. Green and P. M. Naghdi (1992), "On Undamped heat waves in an elastic solid", *J. Therm. Stress.,* 15(2),253-264.

[5] Green, A.E. and Naghdi, P.M. (1993), "Thermoelasticity without energy dissipation", *J. Elast.,* 31(3), 189-209.

[6] Tzou, D.Y. (1995a), "A unified approach for heat conduction from macro-to micro-scales", *J. Heat Transfer.*, 117(1), 8-16.

[7] Tzou, D.Y. (1995b), "Experimental support for the Lagging behavior in heat propagation", *J. Thermophys. Heat Transfer.*, 9(4), 686-693.

[8] Ignaczak, J. (1982), "A note on uniqueness in thermoelasticity with one relaxation time", *J. Therm. Stress.*, 5(3-4), 257–263.

[9] Sherief, H.H. and Dhaliwal, R.S. (1980), "A uniqueness theorem and a variational principle for generalized thermoelasticity", *J. Therm. Stress.*, 3(2), 223–230.

[10] Sherief, H.H. (1987), "On uniqueness and stability in generalized thermoelasticity", *Quart. Appl. Math.*, 45(4), 773–778.

[11] Chandrasekharaiah, D.S. (1998), "Hyperbolic thermoelasticity: A review of recent literature", *Appl. Mech. Rev.*, 51(12), 705-729.

[12] Roy Choudhuri, S.K. (2007), "On A Thermoelastic Three-Phase-Lag Model", *J. Therm. Stress.*, 30(3), 231-238.

[13] Yu, Y.J., Zhang-Na Xue and Xiao-Geng Tian (2018), "A modified Green–Lindsay thermoelasticity with strain rate to eliminate the discontinuity", *Meccanica*, 53, 2543–2554.

[14] Shaw, S. (2020),"A thermodynamic analysis of an enhanced theory of heat conduction model: Extended influence of finite strain and heat flux", *Int. J. Eng. Sci.*, 152, 103277.

[15] Lomakin, A. (1976), "The Theory of Elasticity of Non Homogeneous Bodies", Moscow State University Press, Moscow.

[16] N. Noda (1991), "Thermal stresses in materials with temperature-dependent properties", *Appl. Mech. Rev.*, 44(9), 383-397.

[17] H. M. Youssef (2005), "Dependence of modulus of elasticity and thermal conductivity on reference temperature in generalized thermoelasticity for an infinite material with a spherical cavity", *Appl. Math. Mech.*, 26(4), 470-475.

[18] Xiulin Shen, Kongping Wu, Huanying Sun, Liwen Sang, Zhaohui Huang, Masataka Imura, Yasuo Koide, Satoshi Koizumi, Meiyong Liao (2021), "Temperature dependence of Young's modulus of single-crystal diamond determined by dynamic resonance", *Diamond and Related Materials*, 116, 108403.

[19] Kamiyama, E. and Sueoka, K. (2023), "Method for estimating elastic modulus of doped semiconductors by using ab initio calculations—Doping effect on Young's modulus of silicon crystal", *AIP Advances*, 13(8), 085224.

[20] Yu YJ, Hu W, Tian XG (2014), "A novel generalized thermoelasticity model based on memory-dependent derivative", *Int J Eng Sci.*, 81, 123–134.

[21] Wang, J.L. and Li, H.F. (2011), "Surpassing the fractional derivative: concept of the memory-dependent derivative", *Comput. Math. Appl.*, 62, 3, 1562–1567.

[22] Caputo, M. and Mainardi, F. (1971), "A new dissipation model based on memory mechanism", *Pure and appl. Geophys.*, 91, 134-147.

[23] Abouelregal, A. E., Moustapha, M. V., Nofal, T. A., Rashid, S., and Ahmad, H. (2021). "Generalized thermoelasticity based on higher-order memory-dependent derivative with time delay", *Results in Phys.*, 20, Article: 103705.

[24] Abouelregal, A. E. (2022), “An advanced model of thermoelasticity with higher-order memory-dependent derivatives and dual time-delay factors”, *Waves in Random and Complex Media*, 32(6), 2918-2939.

[25] Kaur, I., Lata, P. and Singh K. (2020), “Memory-dependent derivative approach on magneto-thermoelastic transversely isotropic medium with two temperatures”, *Int J Mech Mater Eng*, 15, 10.

[26] Barak, M.S., Kumar, R., Kumar, R. and Gupta, V. (2023), “The effect of memory and stiffness on energy ratios at the interface of distinct media”, *Multidiscipline Model. Mat. and Struct.*, 19(3), 464-492.

[27] Banerjee, S., Shaw, S., and Mukhopadhyay, B. (2019), “Memory response on thermal wave propagation emanating from a cavity in an unbounded elastic solid”, *J. Therm. Stress.*, 42(2), 294-311.

[28] Jin-Liang Wang, Hui-Feng Li (2021), ”Memory-dependent derivative versus fractional derivative (I): Difference in temporal modeling”, *Journal of Computational and Applied Mathematics*, 384, 112923.

[29] Kaur, I., Singh, K.(2022), “Functionally graded nonlocal thermoelastic nanobeam with memory-dependent derivatives”, *SN Appl. Sci.* 4, 329.

[30] Kaur, I., Lata, P., and Singh, K. (2020), “Effect of memory dependent derivative on forced transverse vibrations in transversely isotropic thermoelastic cantilever nano-Beam with two temperature”, *Appl. Math. Model.*, 88, 83-105.

[31] Kaur, I. and Singh, K. (2021), “Effect of memory dependent derivative and variable thermal conductivity in cantilever nano-Beam with forced transverse vibrations”, *Forces in Mechanics*, 5, 100043.

[32] Shaw, S. (2019),”Theory of generalized thermoelasticity with memory-dependent derivatives”, *Journal of Engineering Mechanics*, 145(3), 04019003.

[33] Ezzat MA, El-Karamany AS, El-Bary AA (2016), “Modeling of memory-dependent derivative in generalized thermoelasticity”, *Eur Phys J Plus.*, 131, Article No.372.

[34] Kumar, R., Tiwari, R., Kumar, R. (2022), ”Significance of memory-dependent derivative approach for the analysis of thermoelastic damping in micromechanical resonators”, *Mechanics of Time-Dependent Materials*, 26(1), 101-118

[35] Gupta, V. and Barak, M.S. (2023), ”Quasi-P wave through orthotropic piezo-thermoelastic materials subject to higher order fractional and memory-dependent derivatives”, *Mechanics of Advanced Materials and Structures*, doi.org/10.1080/15376494.2023.2217420.

[36] Barak, M.S. and Gupta, V. (2023),”Memory-dependent and fractional order analysis of the initially stressed piezo-thermoelastic medium”, *Mechanics of Advanced Materials and Structures*, doi.org/10.1080/15376494.2023.2211065.

[37] Gupta, V., Kumar, R., Kumar, R. and Barak, M.S. (2023),”Energy analysis at the interface of piezo/thermoelastic half spaces”, *Int. J. of Numerical Methods for Heat Fluid Flow*, 33(6), 2250-2277.

[38] Barak, M.S., Kumar, R., Kumar, R. and Gupta, V. (2023), ”Energy analysis at the boundary interface of elastic and piezothermoelastic half-spaces” *Indian J. Phys.*, 97, 2369–2383.

[39] Gupta, V., Kumar, R., Kumar, M., Pathania, V. and Barak, M.S. (2023),”Reflection/transmission of plane waves at the interface of an ideal fluid and nonlocal piezothermoelastic medium”, *Int. J. of Numerical Methods for Heat Fluid Flow*, Vol. 33(2), 912-937.

[40] Yadav, A.K., Barak, M.S. and Gupta, V. (2023),”Reflection at the free surface of the orthotropic piezo-hygro-thermo-elastic medium”, *Int. J. of Numerical Methods for Heat Fluid Flow*, Vol. 33(10), 3535-3560.

[41] Abouelregal, A.E., Ahmad, A., Elagan, S.K. and Alshehri, N.A. (2021),”Modified Moore–Gibson–Thompson photo-thermoelastic model for a rotating semiconductor half-space subjected to a magnetic field”, *Int. J. of Modern Physics C*, 32(12), 2150163.

[42] Abouelregal, A.E., Ahmad, H., Badr, S.K., Elmasry, Y., Yao, S-W. (2022),”Thermo-viscoelastic behavior in an infinitely thin orthotropic hollow cylinder with variable properties under the non-Fourier MGT thermoelastic model”, *Z Angew Math Mech.* 102:e202000344.

[43] Wang, X., and Xu, X. (2001), “Thermoelastic wave induced by pulsed laser heating”, *Appl. Phys.* A, 73(1), 107–114.

[44] Wang, X., and Xu, X. (2002), “Thermoelastic wave in metal induced by ultrafast laser pulses”, *J. Therm. Stress.*, 25(5), 457–473.

[45] Li, Y., Zhang, P., Li, C., and He, T. (2019), “Fractional order and memory-dependent analysis to the dynamic response of a bi-layered structure due to laser pulse heating”, *Int. J. Heat Mass Trans.*, 144, 118664.

[46] Kumar, R., Tiwari, R., Singhal, A. and Mondal, S. (2021), “Characterization of thermal damage of skin tissue subjected to moving heat source in the purview of dual phase lag theory with memory-dependent derivative.”, *Waves in Random and Complex* Media, DOI:10.1080/17455030.2021.1979273.

[47] Al-Qahtani, H. M., and S.K. Datta. (2008), “Laser-generated thermoelastic waves in an anisotropic infinite plate: Exact analysis”, *J. Therm. Stress.*, 31 (6), 569–83.

[48] Shaw, S. and Mukhopadhyay, B. (2017), “A discontinuity analysis of generalized thermoelasticity theory with memory dependent derivatives”, *Acta mech.*, 228, 2675-2689.

[49] M. A. Ezzat, A. El-Karamany, A. A. Samaan (2004), “The dependence of the modulus of elasticity on reference temperature in generalized thermoelasticity with thermal relaxation”, *Appl. Math. Comput.*, 147(1), 169-189.

[50] Shaw, S. and Mukhopadhyay, B. (2013), “Moving heat source response in micropolar half-space with two-temperature theory”, *Continuum Mechanics and Thermodynamics*, 25, 523-535.

[51] G. Honig, U. Hirdes (1984),”A method for the numerical inversion of Laplace transforms”, *J. Comput. Appl. Math.*”, 10(1), 113-132.

[52] Marin, M (1998),”A temporally evolutionary equation in elasticity of micropolar bodies with voids”, *Bull. Ser. Appl. Math. Phys*, 60(3), 3-12.

[53] Marin, M (1998), “Contributions on uniqueness in thermoelastodynamics on bodies with voids”, *Cienc. Mat.* (Havana), 16(2), 101-109.

Contribution of Individual Authors to the Creation of a Scientific Article (Ghostwriting Policy)

- Soumen Shaw and Aktar Seikh carried out the theoretical model and simulation.
- Aktar Seikh has implemented the Algorithm in MatLab.
- Soumen Shaw has organized from the formulation of the problem to the final findings and solution.

Sources of Funding for Research Presented in a Scientific Article or Scientific Article Itself

Author(s) thankfully acknowledges Department of Science and Technology-INSPIRE, Government of India (No. DST/INSPIRE Fellowship/2017/IF170307) for the financial support to carry out this research work.

Conflict of Interest

The authors declare that there is no conflict of interest.

APPENDIX

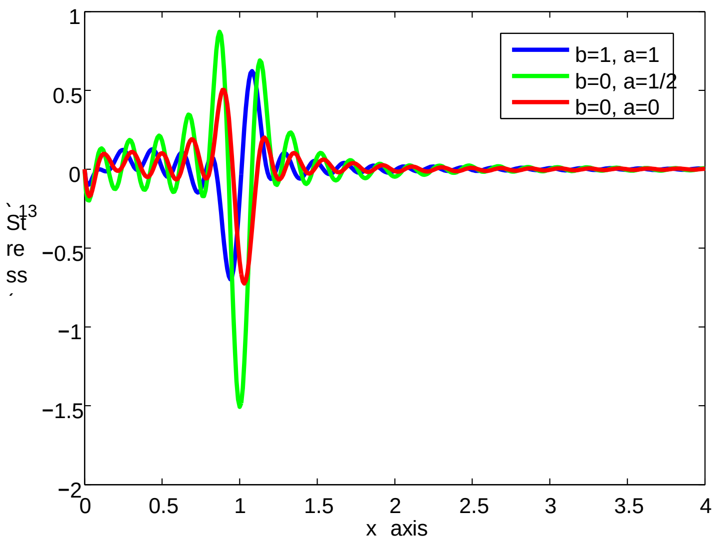

Fig. 1: Shear stress distribution on continuous load for different kernel functions at $t = 0.25$

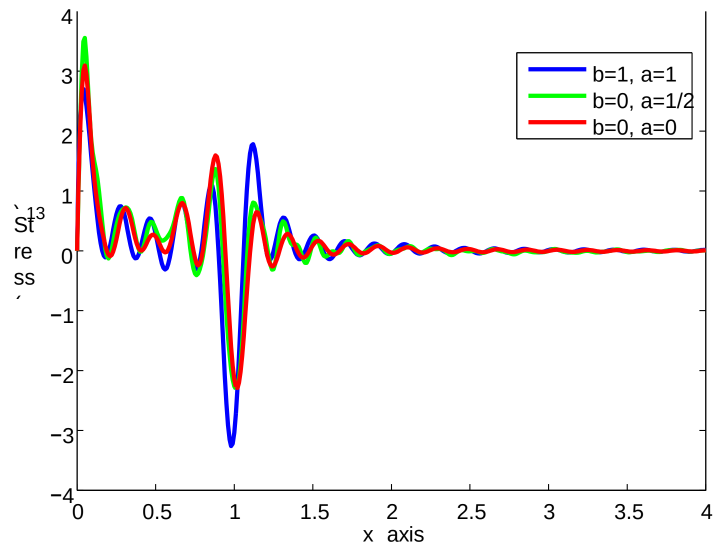

Fig. 3: Shear stress distribution on impact load for different kernel functions at $t = 0.25$

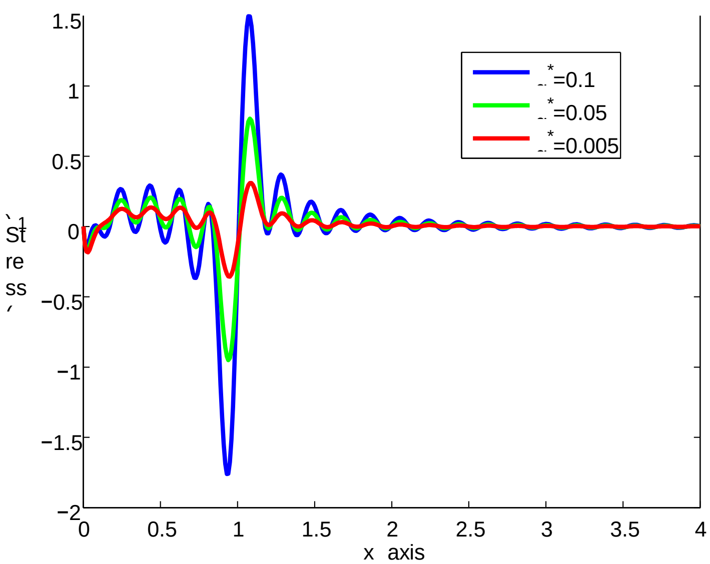

Fig. 2: Shear stress distribution on continuous load for different values of α^* at $t = 0.25$

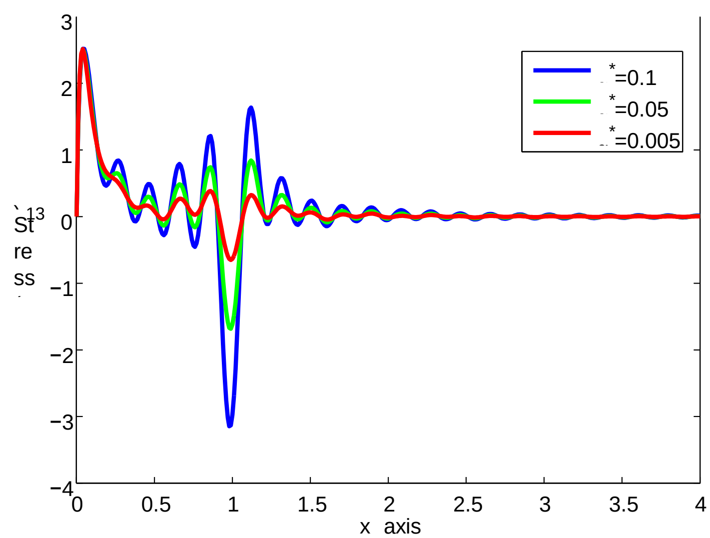

Fig. 4: Shear stress distribution on impact load for different values of α^* at $t = 0.25$

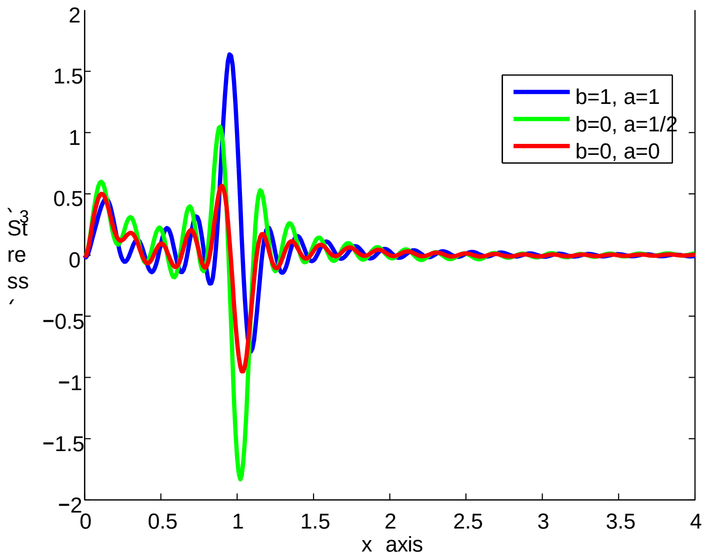

Fig. 5: Normal stress distribution on continuous load for different kernel functions at $t = 0.25$

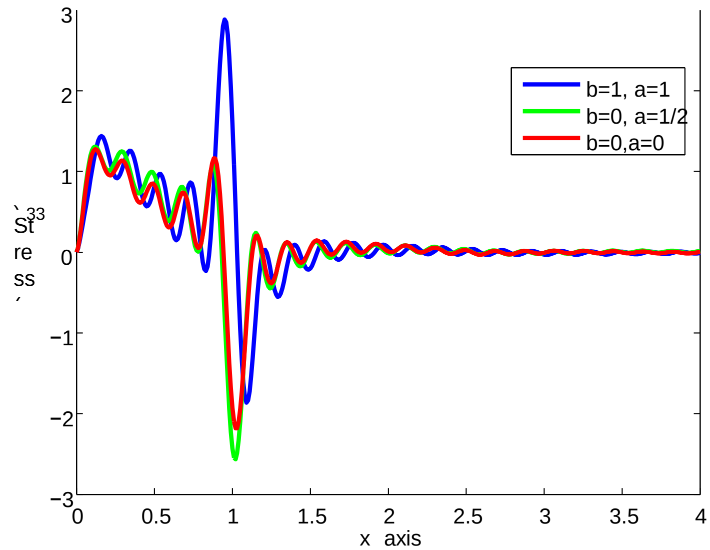

Fig. 7: Normal stress distribution on impact load for different kernel functions at $t = 0.25$

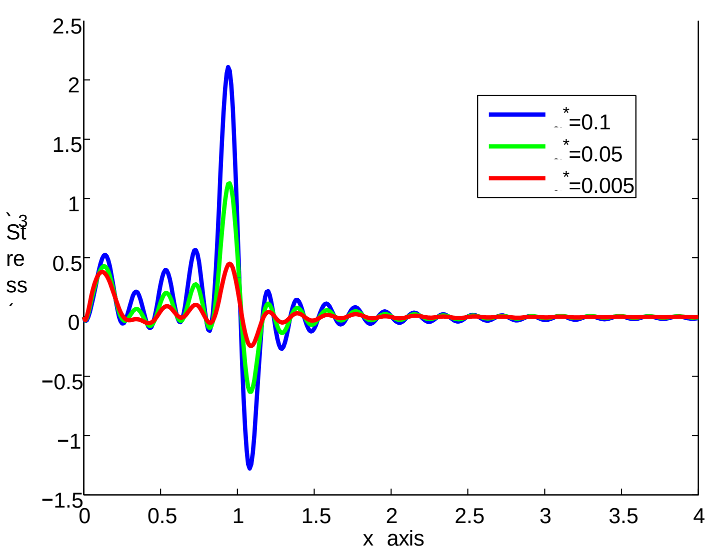

Fig. 6: Normal stress distribution on continuous load for different values of α^* at $t = 0.25$

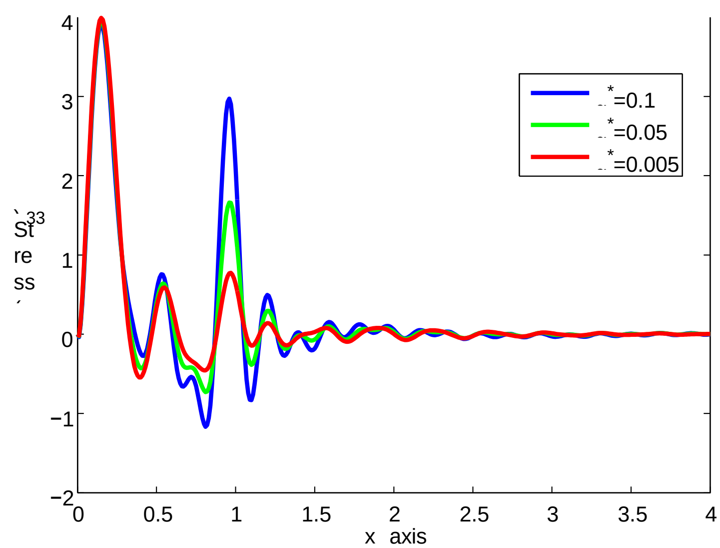

Fig. 8: Normal stress distribution on impact load for different values of α^* at $t = 0.25$

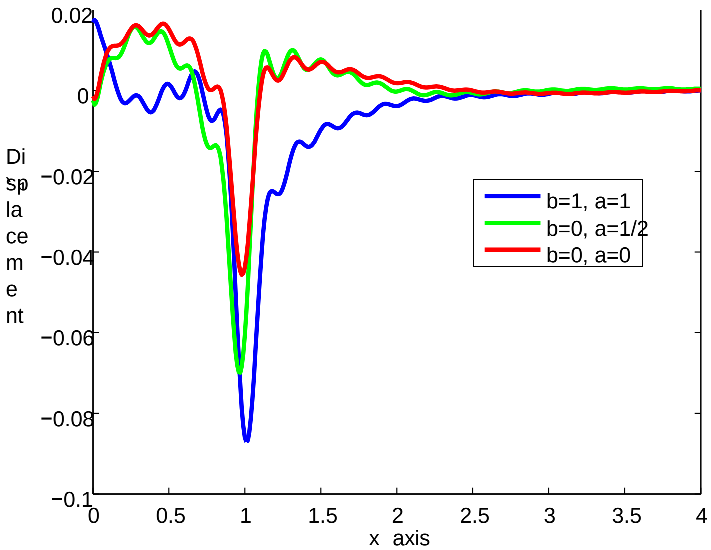

Fig. 9: Displacement component (u_1) on continuous load for different kernel functions at $t = 0.25$

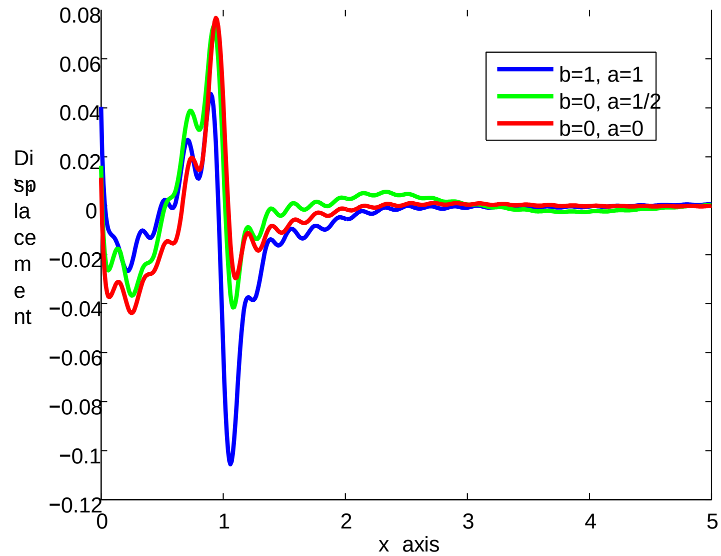

Fig. 11: Displacement component (u_1) on impact load for different kernel functions at $t = 0.25$

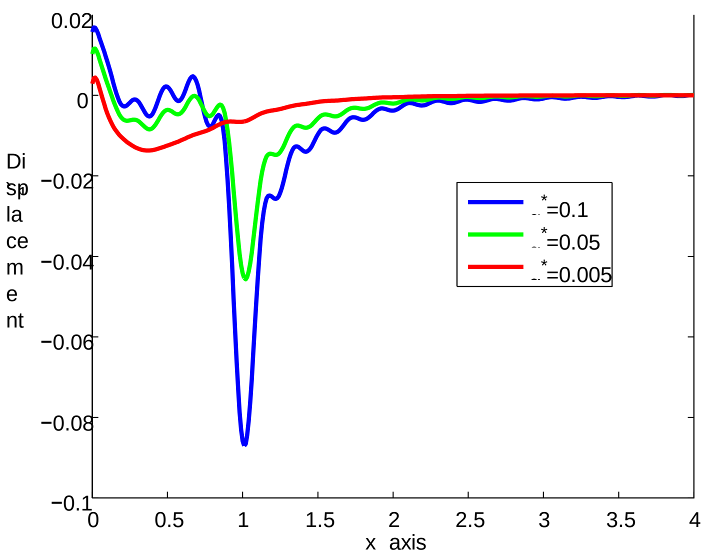

Fig. 10: Displacement component (u_1) on continuous load for different values of α^* at $t = 0.25$

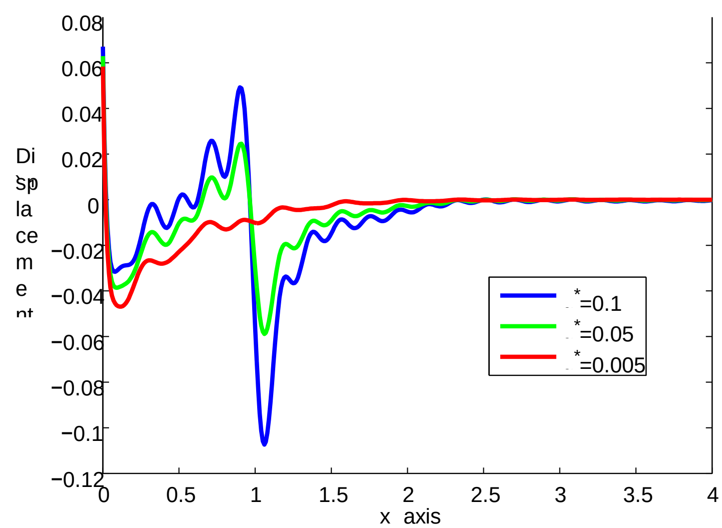

Fig. 12: Displacement component (u_1) on impact load for different values of α^* at $t = 0.25$

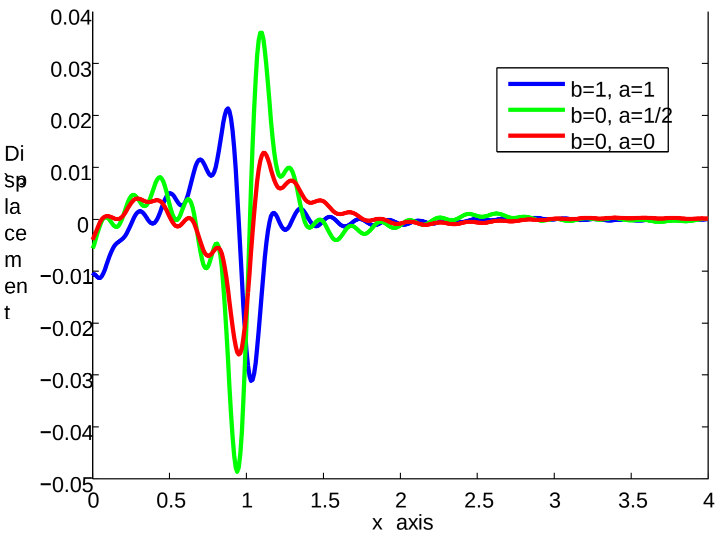

Fig. 13: Displacement component (u_3) on continuous load for different kernel functions at $t = 0.25$

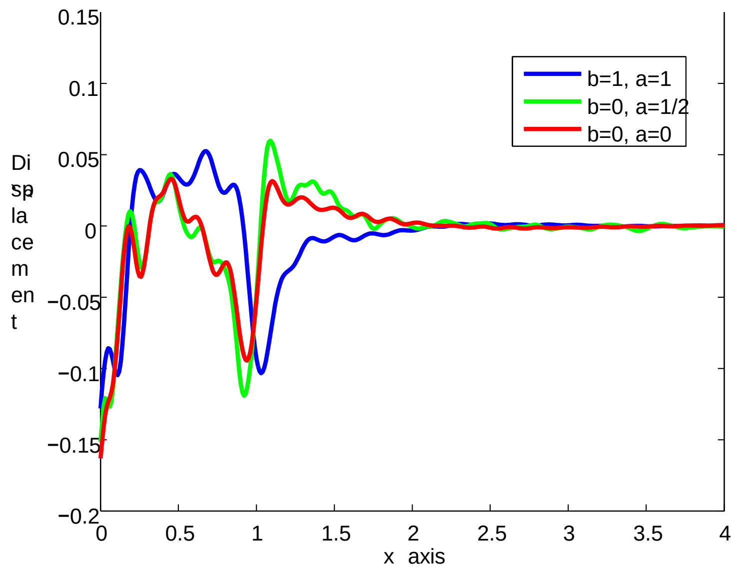

Fig. 15: Displacement component (u_3) on impact load for different kernel functions at $t = 0.25$

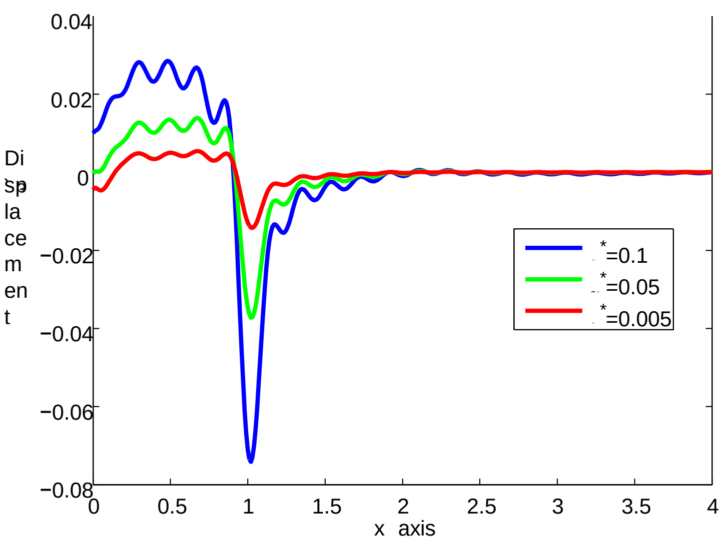

Fig. 14: Displacement component (u_3) on continuous load for different values of α^* at $t = 0.25$

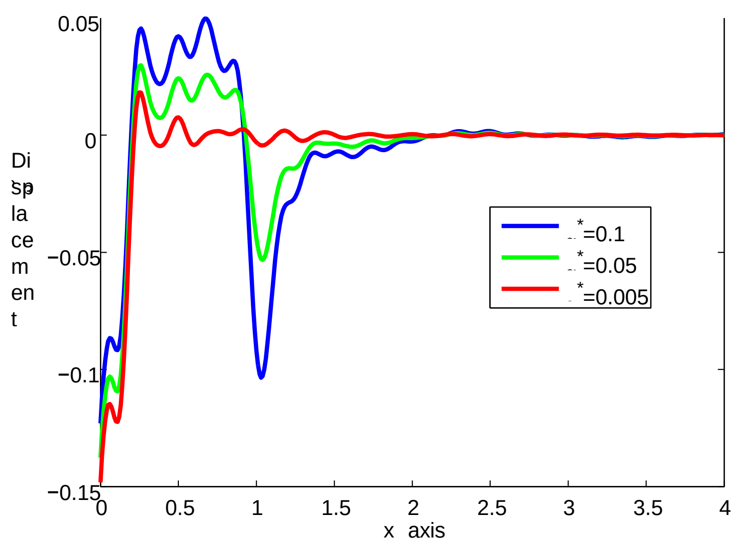

Fig. 16: Displacement component (u_3) on impact load for different values of α^* at $t = 0.25$

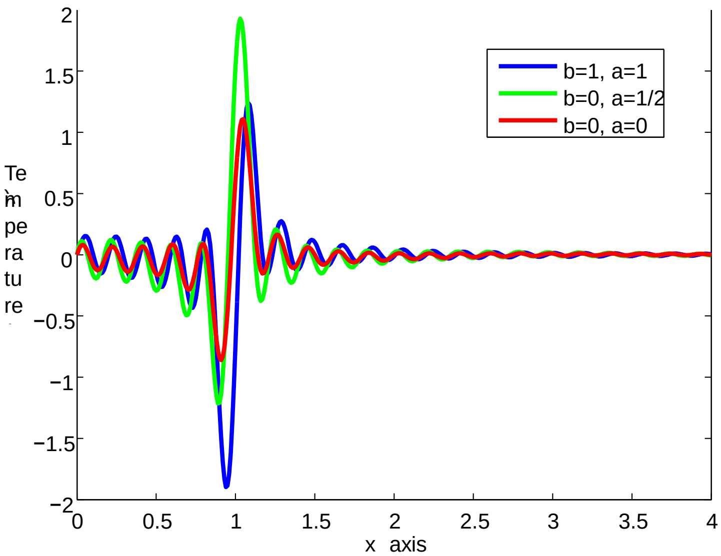

Fig. 17: Temperature distribution on continuous load for different kernel functions at $t = 0.25$

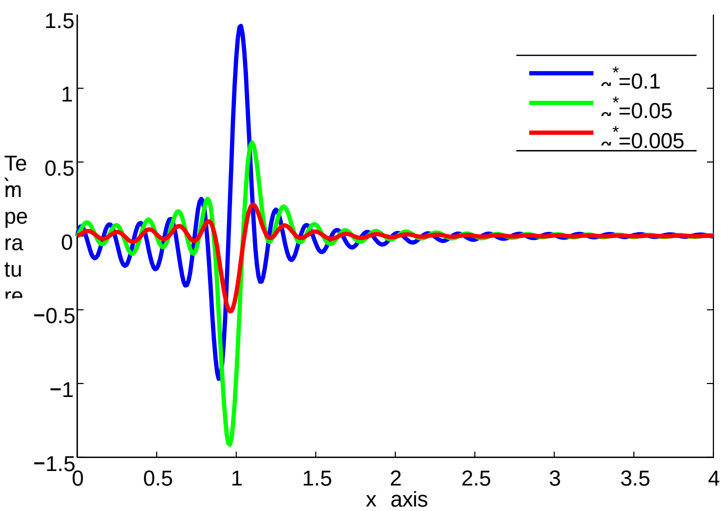

Fig. 18: Temperature distribution on continuous load for different values of α^* at $t = 0.25$

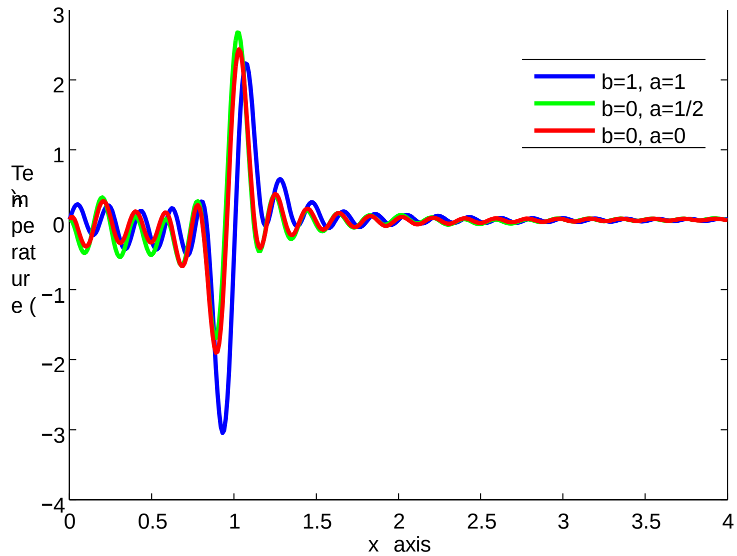

Fig. 19: Temperature distribution on impact load for different kernel functions at $t = 0.25$

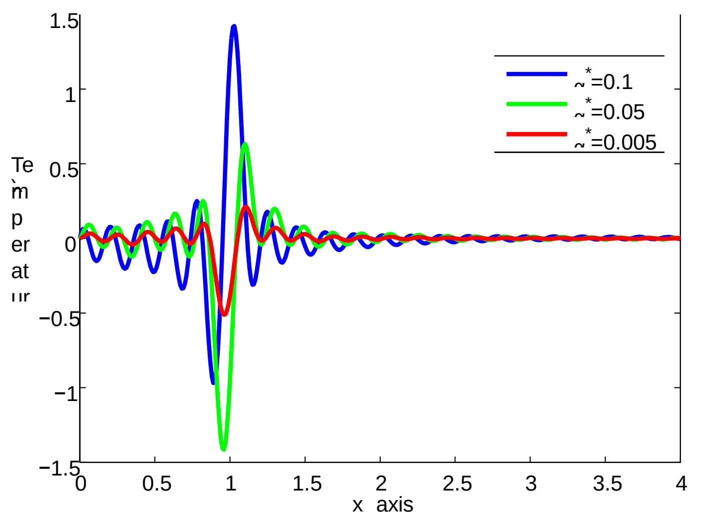

Fig. 20: Temperature distribution on impact load for different values of α^* at $t = 0.25$